OPTIMUM DESIGN FOR BREAKING DEVICE WITH DOUBLE ROLLER BASED EDEM
/
基于 EDEM 的双滚轮破碎装置优化设计

Ruili WANG [1], Deshuai LI [1]; Peiyuan LI [1], Xueyin BAI [1], Tiejun WANG [1], Wei WANG*[1], Yingbo ZHAO[2]
[1]College of Engineering, Shenyang Agricultural University, Shenyang / China
[2]Heishan Chuanqi Agricultural Machinery Equipment Co, Ltd, Jinzhou / China
Tel:18804045818; E-mail: syww@syau.edu.cn
DOI: https://doi.org/10.35633/inmateh-70-55

Keywords: *round bale corn stalks, roller structure, crushing device, numerical simulation*

ABSTRACT

Straw found in the field can be conveniently stored and transported through mechanical packaging, and it undergoes crushing during its utilization. The effectiveness of the crushing process directly impacts the efficiency of material utilization. However, current crushing devices available in the market lack specialized mechanisms suitable for the unique characteristics of round corn stalks. To address this issue, the necessary simulation parameters were determined, and an experiment was conducted using the ternary quadratic combination test method. The test factors considered were the center height difference of the knife roller, lower roller speed, and cutter thickness. The response value of the experiment was the material crushing rate. By analyzing the results, the optimal structural parameters were identified. These included a center height difference of 390 mm for the knife roller, a lower roller speed of 14 r/min, and a cutter thickness of 110 mm. With these parameters, the crushing rate of the round straw crushing device reached 93.77%, and the particle passing ratio was 98.52%. To validate the research findings, a test device was constructed and used to confirm the reliability of the obtained results.

摘要

田间秸秆主要通过机械打包方便进行存储运输,在其使用时进行破碎处理,破碎效果直接影响物料利用效率. 目前,市面上的破碎装置缺乏适用于圆包玉米秸秆物料特性的专用破包装置. 测定必要仿真参数,并基于三元二次组合试验方法进行试验. 确定了以刀辊中心高度差, 下置辊转速和刀具厚度为测试因子,以物料破碎率为测试响应的响应值,得出了最优结构参数,即刀辊中心高度差 390 mm,下置辊转速 14r/min,刀具厚度为 110 mm,此时圆包秸秆破碎装置的破碎率为 93.77%,颗粒通过比例为 98.52%,并据此搭建试验装置验证研究结果可靠.

INTRODUCTION

The utilization of straw bale breaking devices has experienced significant growth, garnering global interest in recent decades. This can be attributed to several factors, including the technique's minimal impact on device structure and the excellent heat production capabilities of straw. The combustion of corn stalks yields a high calorific value, generating heat energy equivalent to 0.5 kg to 0.7 kg of standard coal per 1 kg of dry corn stalk. As a result, straw bale breaking serves as an environmentally friendly, clean, and renewable energy source.

Numerous studies have addressed the mechanical behavior of straw bales at various scales, as documented in the literature *(Bou Ali, 1993; Carrick et al., 1998; King, 2003; Rakowski, 2010; Walker et al., 2004)*. Presently, there are several types of breaking devices in China. However, many of them draw reference from foreign machines, resulting in a considerable disparity between domestic and international situations. Foreign machines are not suitable for our country's circumstances and are costly *(Wen et al., 2020; Yu et al., 2014; Choi et al., 2016; Karayel, D., 2023; Porteus, Sc., 1988; Kornecki, TS., 2022)*. Discrete element simulation technology has been widely employed by scholars both domestically and internationally in the field of agricultural machinery *(Wang et al., 2022; Zhang et al., 2022; Yan et al., 2022; Yu et al., 2020; Liu et al., 2022; Zhou et al., 2022; Feng et al., 2016)*, effectively reducing research and development costs.

This study aims to investigate the mechanical properties and breaking characteristics of round-packed corn stalks using physical experiments and numerical simulations. The structure of the breaking and tearing roller is analyzed to explore the breaking and tearing mechanism of round-packed corn stalks. The findings offer a numerical and theoretical foundation for optimizing the design of mechanical structure parameters, supporting the practical production and processing of round-packed corn stalks.

MATERIALS AND METHODS

Determination of simulation parameters

The focus of this research is the round corn stalks that are collected and packed using the 404Pro type Wittmann round straw baler. Based on the formation principle of round-baled corn stalks, the components of these round-baled stalks consist of intact corn stalks, a significant amount of soil, short stalks, leaves, stalk nodes, and a mixture of soil and silk stalks. The average density of the round corn stalks was measured at 196.08 $\mathrm{kg/m^3}$, with an average moisture content of 16% using the drying method. Due to the irregular nature of conventional physical property measuring equipment and the characteristics of round baled straw materials, it is necessary to conduct scale model tests. The preparation of model materials is one of the main aspects of these tests. Samples were extracted from the original bales of corn stalks and compressed to obtain samples with the same density for testing using the WDW-200 microcomputer-controlled electronic universal testing machine. The test device is mainly PL2-C40C high-speed camera, test plane and lens spacing of 880 mm, the use of high-speed camera on the specimen free fall and rebound process for filming, with a marker pen to mark the bottom edge of the specimen center, to facilitate high-speed camera trajectory to capture and data statistics. In order to ensure the performance effect of recording the falling process, the optimal falling height of the specimen is 370 mm and the distance between the horizontal reference points is 180 mm after several tests.

Determining the collision recovery coefficient between the plate and the device is essential. This coefficient represents an object's ability to deform and return to its original state after a collision. Its value is defined as the ratio of the normal velocity of the object after collision to the normal velocity before collision. It serves as a crucial contact parameter for the simulation test of stacking angles using discrete element simulation software. The test setup, as depicted in Fig. 1, primarily includes the PL2-C40C high-speed camera positioned at a distance of 880 mm from the test plane. The high-speed camera captures the free fall and rebound process of the sample, with a marker pen used to mark the center of the sample's bottom edge. This marking facilitates trajectory capture and data analysis by the high-speed camera. After conducting multiple tests, an optimal falling height of 370 mm and a distance of 180 mm between horizontal reference points were determined to ensure effective recording of the falling process.

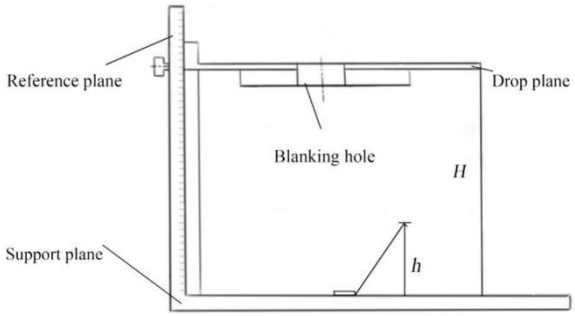

Fig. 1 - Test principle for determination of collision recovery coefficient

Assuming that the sample is only affected by gravity during the falling process, the normal velocity v_1 before the collision and the normal velocity v_2 after the collision are obtained according to the kinetic energy theorem.

$$v_1 = \sqrt{2gh} \tag{1}$$

$$v_2 = \sqrt{2gH} \tag{2}$$

The coefficient of collision recovery

$$\mathrm{e} = \frac{|v_2|}{|v_1|} = \sqrt{\frac{h}{H}} \tag{3}$$

where:

v_1 is the normal velocity before collision, mm·s^{-1}; v_2 is the normal velocity after collision separation, mm·s^{-1}; h is the falling height before collision, mm; H is the maximum height of bounce after collision separation, mm.

The displacement-time curve of the sample's falling and collision rebound process was obtained by utilizing the tracking function of the PLEXLOGplusII high-speed camera analysis software and the drawing function of Origin software. This curve, depicted in Fig. 2, was then applied to equation (3) to determine the collision recovery coefficient between round bundles of corn stalks and between round bundles of straws and

steel plates, based on the selected material of the contact bottom plate. The test process was conducted 10 times to ensure accuracy, resulting in the determination of the collision recovery coefficient between round bundle straw samples and between round bundle straw samples and steel plates. The collision recovery coefficient between round bundle straw samples ranged from 0.3 to 0.4, while that between round bundle straw samples and steel plates ranged from 0.2 to 0.35.

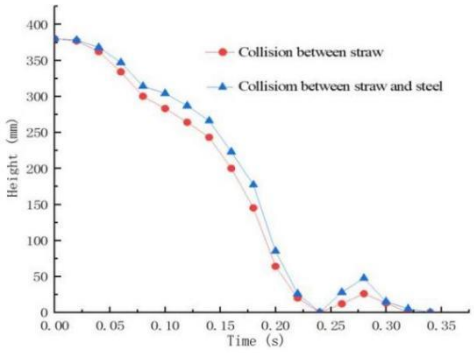

Fig. 2 - Motion displacement-time curve of a corn stalk in round bales colliding with a measured object.

Establishment of discrete element simulation model of corn stalk round bale

The initial step involves establishing the geometric model of the corn stalk round bale. This is accomplished by using Solid-Works to model the bale, which is then saved in x_t format and imported into EDEM. EDEM, developed by DEM-Solutions, Edinburgh, UK, is a CAE software based on the discrete cell method, which is widely used to simulate and study the mechanical properties of particles and the action on particles. (*Luo Shuai et al., 2018*). The Poisson's ratio, shear modulus, and density of the corn stalk round bale are specified, taking into consideration relevant literature, and the static friction coefficient, rolling friction coefficient, and collision recovery coefficient between the geometry and particles are also set. To conduct the discrete element simulation of the breaking process, it is necessary to create models for the particles constituting the round bale. Fig. 3 illustrates the sequence of the physical map of the round bale, the 3D diagram, and the particle bonding diagram, presented from left to right.

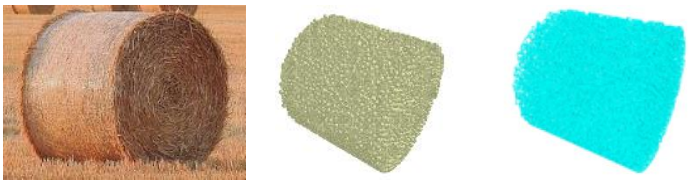

Fig. 3 - Corn stalk round bale

Table 1

Simulation parameters

Material parameters	Numerical value	Geometric parameters	Numerical value
Density [kg/m^3]	189.7	**Density [kg/m^3]**	8864
Poisson's ratio	0.35	**Poisson's ratio**	0.35
Shear modulus	2.01	**Shear modulus**	7.9x10^4
Recovery coefficient between materials	0.37	**Material and geometry recovery coefficient**	0.275
Static friction coefficient between materials	1.22	**Static friction coefficient between material and geometry**	0.465
Rolling friction coefficient between materials	0.54	**Rolling friction coefficient between material and geometry**	0.25

Analysis of influencing factors

By altering the structural and operating parameters of the machine, the working performance of the round straw shredder can be enhanced. Hence, the test variables selected include the center height difference of the counter roller, cutter thickness, number of teeth on a single cutter, rotation speed of the upper roller, and rotation speed of the lower roller. A single-factor simulation test is conducted, with the material crushing rate serving as the evaluation index.

Through the analysis of variance, it becomes possible to explore the contribution of variations from different sources to the overall variation and further determine the influence of experimental factors on the evaluation index.

The test levels are determined based on theoretical calculations and a thorough review of relevant literature, as presented in Table 2.

Table 2

Factors and levels of single factor test

Experimental factors	Levels						
Counter roller height difference [mm]	0	195	390	585	780	975	1170
Single tool tooth number	5	6	7	8	9		
Tool thickness [mm]	70	80	90	100	110		
Top roller speed [rpm]	10	12	14	16	18		
Lower roller speed [rpm]	10	12	14	16	18		

Based on the relevant literature and the actual characteristics of broken round corn stalks, the unnecessary materials for composite crushing were carefully weighed. As a result, the average crushing rate achieved by the round corn stalk crusher was found to be 85%, aligning with the findings of previous research conducted by the enterprise.

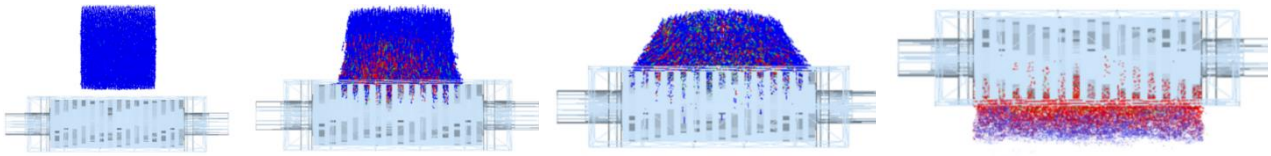

Fig. 4 - Simulation process of round corn stalk crushing

Influence of the number of cutter teeth on the broken rate of straw

The optimal conclusions drawn from the one-way test in Table 2 are described below. The upper roller operates at a rotation speed of 16 r/min, while the lower roller rotates at 14 r/min. The center height difference is set to 585 mm, the cutter thickness is 80 mm, and the number of teeth varies between 5, 6, 7, 8, and 9. A total of five groups of simulation tests are conducted, and the results are depicted in Fig. 5. The experimental findings indicate that the number of cutter teeth has a significant influence on the straw crushing rate ($P > 0.05$). However, it does not have a significant impact on the material crushing rate. Notably, when the experimental factors consist of eight teeth, the material crushing rate of the material block is higher, and the trend of the crushing rate remains relatively consistent throughout the simulation time. On the other hand, when the number of teeth is five, the crushing rate is the lowest, resulting in the poorest crushing effect. Furthermore, the change in material crushing rate is similar between 2 to 3 s when the number of teeth is six. However, there is a significant reduction in material crushing rate during the intervals of 0 to 2 s and 3 to 4.2 s. Although the number of cutter teeth exhibits an increasing trend in material breakage rate, the rate of increase is not substantial. Consequently, the number of cutter teeth is not considered as an investigated factor in the subsequent multi-factor test.

The verification test was conducted following the test method outlined in relevant references (*Yang Tao et al., 2017*), using the material crushing rate as the test index. Crushing rate refers to the percentage of the mass of the material required for composite crushing to the total mass of the original material after crushing treatment, and the ratio of bond breaking is used as the evaluation index of the crushing rate in the simulation test, which is determined by Formula 4.

$$p_p = \frac{n}{N} \times 100\% \quad (4)$$

where:

P_p is material crushing rate, %; n is number of bond breaks; N is total number of bonding keys.

The productivity was calculated using Formula 5.

$$E_0 = \frac{m}{T \cdot p_1} \times 60 \quad (5)$$

where:

E_0 is productivity, kg/(kW·h); P_1 is the total mass of materials, kg; T is Time, min; m is quality, kg.

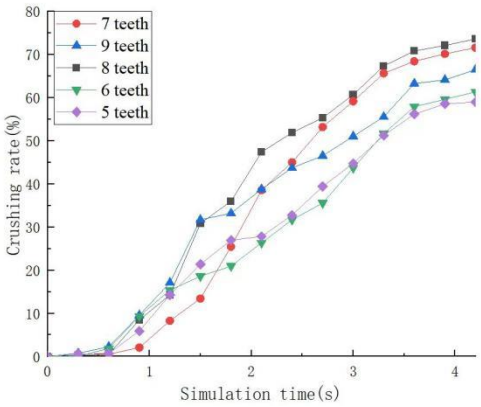

Fig. 5 - Variation curve of particle crushing rate with different cutter teeth

The influence of cut thickness on straw crushing rate

The parameters for the round straw shredder are determined as follows: the rotation speed of the upper roller is 16 r/min, the lower roller is 14 r/min, the center height difference is 585 mm, the number of teeth is 7, and the thickness ranges from 70 to 110 mm with intervals of 10 mm. Five sets of simulation tests are conducted, and the results are presented in Fig. 6. The experimental findings reveal that the thickness of the cutter has a significant impact on the straw crushing rate ($P < 0.05$) as well as the material crushing rate. With the rotation speeds of the upper and lower cutter rolls and the center height difference of the cutter roll kept constant, it is observed that variations in the inner blade thickness between 70 and 80 mm do not significantly affect the test results. However, when the thickness reaches 90 mm, the crushing rate is lower within the 1 to 3-s range compared to other thickness ranges. As the simulation time increases to 3 to 4.2 s, the crushing rate tends to peak at different tool thicknesses. Consequently, the tool thickness can be considered as an investigated factor in the subsequent multi-factor test.

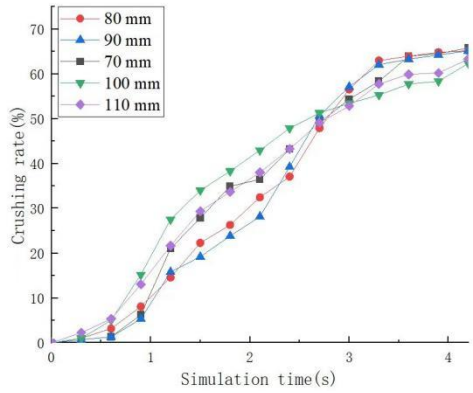

Fig. 6 - Variation curve of particle crushing rate with varying tool thicknesses.

The influence of rotation speed of lower roll on straw crushing rate

A series of simulation tests are conducted with different parameters: the rotation speed of the upper roller is set at 16 r/min, the number of cutter teeth is 7, the center height difference is 585 mm, the cutter thickness is 80 mm, and the rotation speed of the lower roller varies between 10, 12, 14, 16, and 18 r/min. The results of these tests are depicted in Fig. 7. The experimental findings demonstrate that the lower roller speed has a significant influence on the straw crushing rate ($P < 0.05$) and also affects the material crushing rate. When the rotation speed of the lower roller is set at 12, 14, and 16 r/min, the material crushing rate remains relatively stable, outperforming the rates obtained at other rotation speeds. Notably, the highest material crushing rate is achieved at 14 r/min, reaching 82.85%. In contrast, when the rotation speed is 10 r/min, the material crushing rate is significantly lower at 66.86% compared to the rates obtained at other rotation speeds, indicating a relatively poor crushing effect. It is evident that the rotation speed of the lower roller exerts a substantial influence on the material crushing rate, and the rate notably increases within the 1 to 3-s interval as the rotation speed of the lower roller increases. Therefore, the rotation speed of the lower roller will be investigated further as a factor in subsequent multi-factor tests.

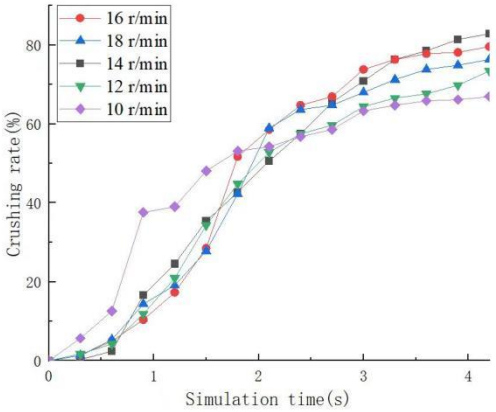

Fig. 7 - Variation curve of particle crushing rate with varying lower roller speeds.

The influence of rotation speed of the top roller on straw crushing rate

It has been established that the rotation speed of the lower roller is 14 r/min, the number of teeth is 7, the center height difference is 585 mm, the tool thickness is 80 mm, and the rotation speed of the upper roller varies between 10, 12, 14, 16, and 18 r/min. Five sets of simulation tests are conducted, and the results are displayed in Fig. 8. The experimental findings indicate that the top roller speed has a significant influence on the straw crushing rate ($P > 0.05$) but does not significantly affect the material crushing rate. Higher rotation speeds of the upper roller, such as 16 and 18 r/min, result in higher material crushing rates, with a trend that aligns with the simulation time. Conversely, a rotation speed of 10 r/min yields the lowest material crushing rate, indicating poor material crushing effectiveness. The change in material crushing rate between 2 and 3 s is comparable to that at 14 r/min; however, the crushing effect is worse than other rotation speeds during the intervals of 0–2 s and 3–4.2 s. Consequently, it is observed that the material crushing rate increases with an increase in the speed of the upper roller, but the impact is not significant. As a result, the rotation speed of the upper roller is not considered an investigated factor in the subsequent multi-factor test.

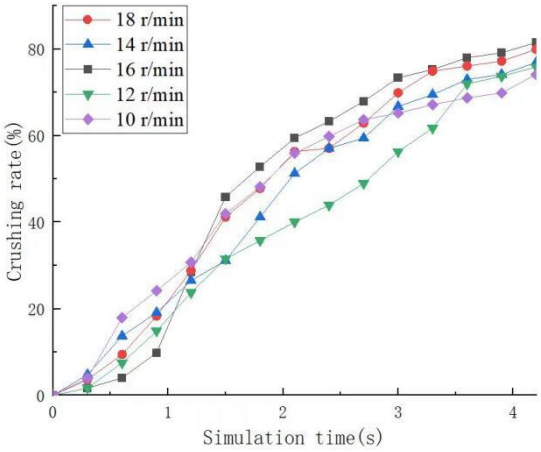

Fig. 8 - Variation curve of particle crushing rate with different rotating speeds of the upper roller

The influence of height difference of knife roll center on straw crushing rate

It is established that the rotation speed of the upper roller is 16 r/min, the lower roller is 14 r/min, the number of teeth is 7, the cutter thickness is 80 mm, and the height difference between the centers of the two cutter shafts varies between 0, 195, 390, 585, and 780 mm. Five sets of simulation tests are conducted, and the results are illustrated in Fig. 9. The experimental findings reveal that the difference in center height of the knife roller has a significant impact on the straw crushing rate ($P < 0.05$) and also influences the material crushing rate. When the height difference between the centers of the two rollers is 390 mm, the material crushing rate reaches its highest value at 82.0%. When the height difference is 195 mm and 585 mm, the change in crushing rate shows no significant variation, and the rates are recorded as 73.4% and 76.3%, respectively. When the center height difference is 0 mm, the material crushing rate is notably lower compared to the rate at 390 mm, and the lowest peak value of the material crushing rate is observed at 780 mm, with a rate of only 66.9%.

Furthermore, when the center height difference is 0, 195, 390, 585, and 780 mm, the material crushing rate exhibits a trend of initially increasing and then decreasing, with the best effect observed when the center height difference ranges from 195 to 585 mm. Consequently, the center height difference of the knife roller is considered an investigated factor in the subsequent multi-factor test.

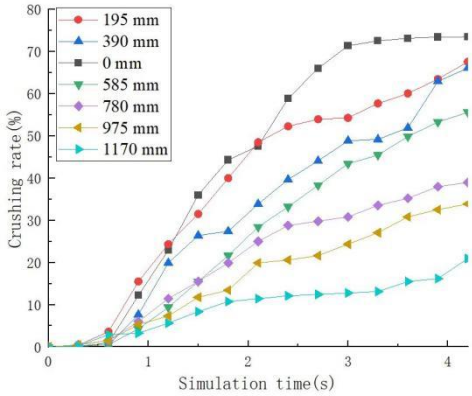

Fig. 9 - Variation curve of particle crushing rate with different center height.

The aforementioned test results demonstrate the significant influence of the center height difference, cutter thickness, and lower roller speed on the material crushing rate ($P < 0.05$). These factors can be considered as important variables for subsequent multi-factor tests.

Scheme design and result analysis of combined test

Test Purpose

(1) To assess the rationality of the structure of the double-roller differential round-baled corn stalk shredder used in this research, and evaluate if the key components meet the specified requirements.

(2) To verify if the crushing efficiency of the shredding device meets the design criteria and desired efficiency.

(3) To determine the optimal structural parameters for the shredding device of the double-roller differential round-baled corn stalk shredder.

Test method and evaluation index

(1) Material crushing rate: This term pertains to the proportion of the required material mass for composite crushing within a single workflow in relation to the total material mass.

(2) Particle passing ratio: This concept indicates the percentage of particles passing through the discharge port within a single workflow relative to the total number of particles in the entire model. Its calculation formula is represented by Formula 6.

$$p_t = \frac{s}{S} \times 100\% \quad (6)$$

where:

P_t is particle passing ratio; s refers to the number of particles passing through a single operation, one; S is total number of particles.

Particle Passing Ratio: is the percentage of the number of particles passing through the outlet in a single workflow compared to the number of particles in the entire model.

Test model

The traditional shredding device exhibits inadequate crushing effectiveness on round straw, with issues such as uneven distribution of cutter utilization benefits and significant loss of certain cutters. To address these concerns, a differential crushing method utilizing two rollers is proposed. This method involves crushing round straw through the relative rotation of the crushing cutter roller, while simultaneously enabling automatic transportation due to the substantial mass of the straw itself, thereby enhancing work efficiency. The differential-roller-type bale breaking device is employed to break and preliminarily crush round-packed corn stalks, facilitating subsequent processing. Optimizing the design of the round-packed straw shredding device is instrumental in improving the effective utilization rate of round-packed corn stalks. To achieve this, the following design requirements are presented for the shredding device:

(1) The straw material should be effectively and preliminarily broken, ensuring a successful bag-breaking outcome.

(2) The bag-breaking device should be equipped with a motor capable of meeting production requirements through the designed rotation speed.

(3) The occurrence of blockages should be avoided.

(4) The preliminarily crushed material should meet the processing and application requirements, such as achieving a crushing rate of 60% for incineration power generation.

(5) The cutter chamber of the device should possess a simple structure, exhibit high working efficiency and reliability, and maintain optimal working conditions continuously.

The frame is connected to the bottom of the motor and the bottom of the reducer through connecting plates on both sides, while the top of the steel structure in the middle of the frame is fixedly connected to the bottom of the cutter chamber main body using connecting plates. One end of the motor's output shaft is firmly connected to one end of the reducer's input shaft through a coupling, and the other end of the reducer's output shaft is fixedly connected to the cutter shaft via a coupling. The cutter shaft extends from the reducer through the machine body and is rotatably connected to one side of the inner wall of the cutter chamber body using a bearing. The outlet is axially secured with an end cover. On the inner surface of the cutter shaft within the main body of the chassis, the cutter and spacer are firmly attached. A second cutter shaft, positioned symmetrically with the first cutter shaft along the centerline, is mounted between the two sides of the inner wall of the chassis and on one side of the cutter shaft. The two shafts extend through the machine body to one side of the chassis. There is no noticeable difference between the top and bottom of the chassis body. Typically, the top surface is used as the inlet, and the bottom as the outlet. The distance between the center lines of the cutter shafts measures 420 mm, as depicted in Fig. 10, when compared to the actual equipment.

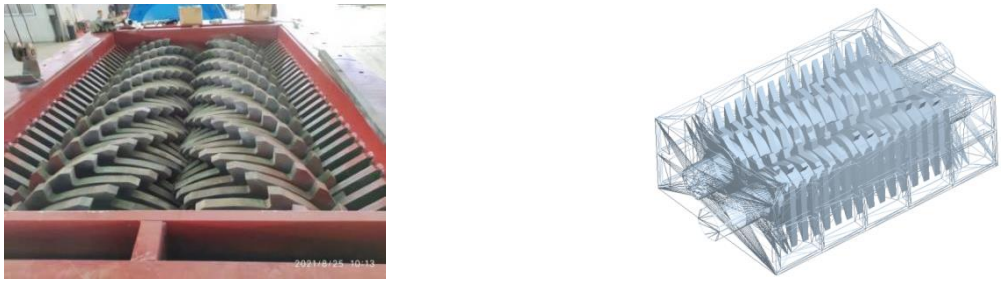

Fig. 10 - Shredding device comparison diagram

After analyzing the results of the single-factor tests and reviewing relevant literature, three significant factors were identified for further investigation: the height difference of the cutter roller center, the cutter thickness, and the rotating speed of the lower roller. The evaluation indexes used were the crushing rate of the round-packed corn straw material model and the particle passing ratio in a single operation. Taking into account the device design and the results of the single-factor tests, and considering real-world working conditions, the levels of the various factors were determined as outlined in Table 3.

Table 3

Test factor level table

level	parameter		
	Center height difference[mm]	Tool thickness[mm]	Lower roller speed[rpm]
-1	195	90	12
0	390	100	14
1	585	110	16

RESULTS

Test scheme and results

Based on the findings from previous single-factor simulation tests and relevant research on differential roller equipment both domestically and internationally, and considering the practical production requirements, the following parameters have been determined: the rotational speed of the upper cutter roller is set at 16 r/min, while the lower cutter roller's speed ranges from 10 to 16 r/min.

The cutter thickness is set between 70 mm and 110 mm to align with operational needs, and the number of cutter teeth is fixed at 7. Additionally, considering the material's structural characteristics and test results, the optimal range for the height difference between the centers of the two rollers is established as 70 mm to 90 mm.

By assessing the significance of each index and establishing the relationships among the factors, the optimal parameter combination for the roller differential speed package breaking equipment has been determined. The test factors are represented by the codes shown in Table 4, and the corresponding test results are presented in Table 5. X_1, X_2, and X_3 denote the coded values of the factors.

Table 4

Test scheme and results

No.	Center height difference / [mm]	Tool thickness / [mm]	Lower roller speed / [rpm]	Material crushing rate / [%]	Particle passing ratio / [%]
1	-1	-1	0	86.24	96.07
2	-1	1	1	88.99	95.44
3	1	0	1	89.46	97.3
4	-1	0	-1	90.77	95.73
5	0	1	-1	89.34	97.52
6	1	0	-1	87.84	95.14
7	0	0	0	88.99	96.47
8	1	0	-1	84.54	95.46
9	0	0	0	91.1	96.74
10	0	0	0	90.24	97.46
11	0	0	0	93.31	98.02
12	0	-1	1	92.17	97.1
13	0	0	0	92.21	96.67
14	-1	1	0	88.01	94.76
15	1	-1	0	90.31	96.64
16	0	0	0	90.12	98.01
17	0	1	1	93.48	98.62

Table 5

Significance test results of regression relationship of material crushing rate

Source of variation	Sum of square	Degree of freedom	Mean square	F value	P value	Significance
Model	66.31	9	7.37	5.63	0.0164	*
X_1	8.29	1	8.29	6.34	0.0399	*
X_2	1.35	1	1.35	1.03	0.3429	
X_3	4.82	1	4.82	3.69	0.0963	
X_1X_2	4.49	1	4.49	3.44	0.1062	
X_1X_3	11.22	1	11.22	8.58	0.0220	*
X_2X_3	2.71	1	2.71	2.07	0.1935	
X_1^2	24.81	1	24.81	18.97	0.0033	**
X_2^2	3.66	1	3.66	2.08	0.1382	
$X_1X_2^2$	11.66	1	11.66	8.92	0.0203	*
Residual	9.15	7	1.31			
Lack of Fit	1.76	3	0.59	0.32	0.8113	
Pure Error	7.38	4	1.84			
Sum	75.46	16				

Establishment of Regression Model and Analysis of Variance

As shown in Tables 5 and 6, the regression coefficient test results reveal significant effects of the primary term X_1 and the quadratic terms X_1X_3 and $X_1X_2^2$ on crushing rate X ($P < 0.05$). Additionally, the quadratic term X_1^2 exhibits an extremely significant effect on crushing rate X ($P < 0.01$). Furthermore, the quadratic term $X_1^2X_2$ has a significant effect on the particle passing ratio Y ($P < 0.05$), and the quadratic term X_1^2 significantly affects the particle passing ratio Y ($P < 0.01$). From Tables 4–4 and 4–5, it can be observed that the model's p-value for crushing rate X is 0.0164, and the p-value for the particle passing ratio Y is 0.0174. Both values are less than 0.05, indicating the significance of the model. On the other hand, the missing items have p-values of 0.8113 and 0.9201, respectively, which exceed 0.05, suggesting their lack of significance.

The difference between the determination coefficient R^2 and the adjusted R-squared (R_{Adj}^2) is less than 0.2, confirming the reliability of the model. Consequently, the regression model can effectively analyze and predict the data related to the test target.

Table 6

Results of significance test of regression relationship of particle passing ratio

Source of variation	Sum of square	Degree of freedom	Mean square	F value	P value	Significance
Model	13.66	9	1.52	5.51	0.0174	*
X_1	0.99	1	0.99	3.61	0.0994	
X_2	0.44	1	0.44	1.58	0.2490	
X_3	0.38	1	0.38	1.39	0.2771	
X_1X_2	0.01	1	0.01	0.03	0.8615	
X_1X_3	0.86	1	0.86	3.10	0.1215	
X_2X_3	0.15	1	0.15	0.55	0.4818	
X_1^2	8.17	1	8.17	29.66	0.0010	**
X_2^2	0.46	1	0.46	1.66	0.2389	
$X_1^2X_2$	2.13	1	2.13	7.73	0.0273	*
Residual	1.93	7	0.28			
Lack of Fit	0.20	3	0.068	0.16	0.9201	
Pure Error	1.73	4	0.43			
Sum	15.61	16				

Influence of interaction of test factors on response index

To provide a more visual representation of the interaction among the test factors, response surface analysis of the regression model was conducted using Design Expert software. The resulting response surface charts, shown in Fig. 11 and 12, illustrate the impact of the interaction between the center height difference of the cutter roller, the cutter thickness, and the rotation speed of the lower roller on both crushing rate and the particle passing ratio. By setting one of the factors to zero and analyzing the influence of the other two factors on crushing rate and particle passing ratio, the response surface analysis reveals the trend and effect of each factor on the test results.

The influence of various factors on crushing rate is shown in Fig. 11.

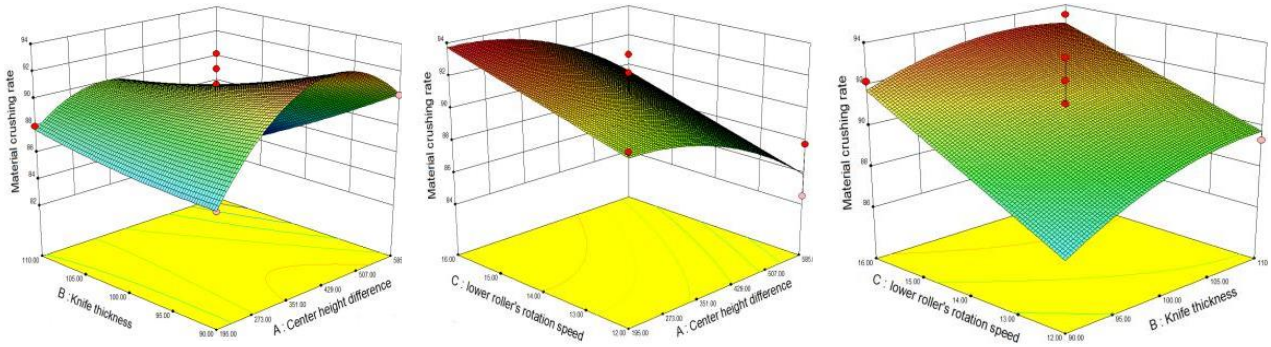

Fig. 11 - Effect of interaction of factors on bond fracture rate

Fig. 11 illustrates the impact of the interaction between the center height difference of the cutter roller and the cutter thickness on the bonding fracture rate, with the rotation speed of the lower roller set at the central value. As the center height difference increases and the cutter thickness decreases, the bonding fracture rate initially increases and then decreases. Similarly, the interaction between the center height difference of the cutter roller and the rotation speed of the lower roller influences the bonding fracture rate, with an increasing trend observed as the difference in center height and rotation speed increases. Likewise, when considering the interaction between the cutter thickness and the rotation speed of the lower roller, a higher bonding fracture rate is observed as the cutter thickness and rotation speed decrease.

The response surface depicting the influence of each factor on the particle passing ratio is displayed in Fig. 12.

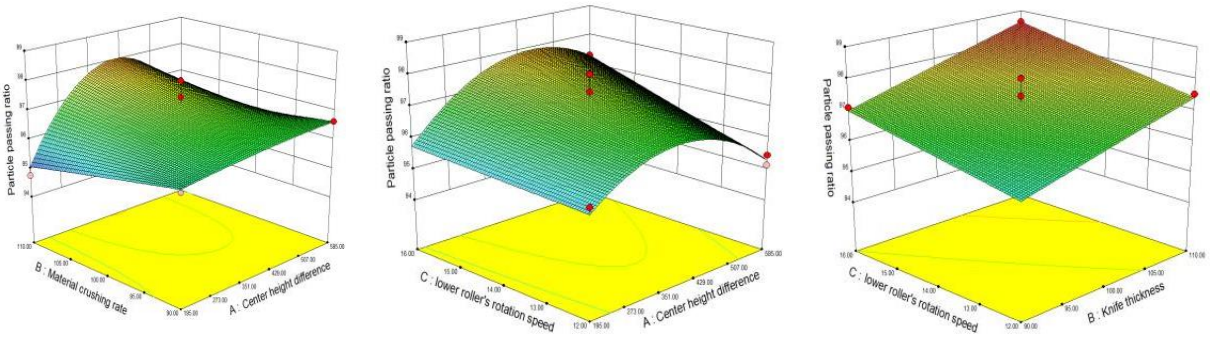

Fig. 12 - Effect of interaction between factors on particle passing ratio.

Fig. 12 illustrates the impact of the interaction between the center height difference of the knife roller and the knife thickness on the particle passing ratio when rotation speed of the lower roller is at the center position. As the height difference between the center of the cutter roller increases and the cutter thickness decreases, the particle passing ratio initially increases and then decreases. Similarly, the interaction between the height difference of the cutter roller center and the rotation speed of the lower roller influences the particle passing ratio, showing an increasing trend as the height difference and rotation speed increase. Furthermore, the interaction between the cutter thickness and the rotation speed of the lower roller affects the particle passing ratio, with a decreasing cutter thickness and an increasing rotation speed leading to an upward trend in the particle passing ratio.

Parameter optimization and verification

By considering the height difference between the center of the cutter roller (X_1), the thickness of the cutter head (X_2), and the rotation speed of the lower roller (X_3) as constraints, and the number of bond breaks (X) and the particle passing ratio (Y) as objectives, a structural optimization parameter model for the round corn stalk breaking device is established. The calculation method for the model is presented in Formula7.

$$\begin{cases} maxX \\ maxY \\ 195 \le X_1 \le 585 \\ 70 \le X_2 \le 110 \\ 12 \le X_3 \le 16 \end{cases} \quad (7)$$

After optimizing the regression equation, the optimal combination of parameters for the round corn stalk breaking device is determined as follows: a height difference of 390 mm between the center of the cutter roller, a cutter head thickness of 110 mm, and a rotation speed of the lower roller at 14 r/min.

Based on the optimized parameter combination, a crushing test is conducted on the straw round bale. Through analysis of the test results, the Design-Expert software is utilized to further optimize the three test factors within their respective ranges. The optimal process parameters are determined as follows: a center height difference of 390 mm, a cutter thickness of 110 mm, and a lower roller speed of 14 r/min.

Under these optimal conditions, the shredder achieves the best crushing effect, with a bond crushing rate of 93.48% and a particle passing rate of 98.62%. The details of the test scheme can be found in Table 7.

Table 7

Results of significance test of regression relationship of particle passing ratio

Name	value
Center height difference of knife roller [mm]	390
Cutter head thickness [mm]	110
Lower roller speed [rpm]	14

The experiment was conducted three times using the optimal parameter combination, and the crushing rate and working efficiency rate of the material were measured. The average values were calculated, resulting in a crushing rate of 93.77% and a working efficiency of 98.52%. The prediction deviation between the experiment and the model described above is within 5%, indicating the reliability of the regression model.

Then with crushing five round-packed corn stalks, the following conclusions were drawn:

Five rounds of bench tests were conducted to crush round-packed corn stalks, and the figure illustrates the comparison between the crushed materials and the simulation results.

The material crushing rates were 94.63%, 93.95%, 95.12%, 92.16%, and 94.01%, respectively, with an average of 93.97%. Using the simulation test results as a benchmark, the results were subjected to a T-test in Origin software, yielding a P-value of 0.705 (>0.05), confirming the reliability of the test results. The productivity values were 5125.7 kg/h, 5336.2 kg/h, 5203.1 kg/h, 5107.4 kg/h, and 5259.6 kg/h, respectively, with an average of 5206.4 kg/h. Compared to the traditional double-roller structure, the double-roller differential corn stalk round bale breaking device proposed in this study demonstrates improvements in material crushing rate and productivity.

CONCLUSIONS

In this study, a breaking device based on double-roller structure was designed considering the unique external surface profiles and interior tissue of straw bale, combined with knowledge of agricultural mechanics, agricultural engineering, materials science, and other fields.

Straw bale was broken during the bale-breaking period, and the bale breaking model was established in stages. The accuracy and scientific nature of the model were verified by comparing the breaking rate collected from conventional breaking with experimental data.

(1) Compared with the existing breaking device, the breaking device with double-roller studied in this paper has the following advantages. A ternary quadratic combination experiment was conducted to determine the best structural parameters of the shredding device for the roller differential round corn stalk shredder. The regression equation was derived, along with an assessment of its impact on the results. The optimal parameters, including a center height difference of 390 mm, tool thickness of 110 mm, and lower roller speed of 14 r/min, were determined and validated through bench testing. Simultaneously, various control groups were established and applied in the subsequent simulation tests to verify the superiority of this structure.

(2) The model parameters of the straw bundle were determined by the factor test. The optimal parameters, including a center height difference of 390 mm, tool thickness of 110 mm, and lower roller speed of 14 r/min, were determined and validated through bench testing. The more the deviation from the above data, the less accurate the results will be. Therefore, a ternary secondary combination experiment was conducted. By defining a reasonable calculation domain in the EDEM calculation could reduce the calculation time without affecting the whole.

(3) This design method can be applied to the design of other breaking parts of agricultural machinery. This approach is not limited to straw bales and has strong generality to solve the problem of efficient utilization of straw. In order to make better use of agricultural mechanics to solve the problem of straw utilization, a database matching a variety of straw organisms with the actual production conditions of more agricultural machinery will be established in the future, so as to provide more inspirations for the design of agricultural machinery from the perspective of agricultural mechanization. This method ignores the anisotropy of components in straw bale because only breaking rate of straw bale was analyzed in this study. Therefore, to make our model closer to the actual soil environment, the next steps will be to add the characteristic parameters of the straw breaking force caused by interior components and to perform further exploration by coupling the ANSYS and EDEM methods.

ACKNOWLEDGEMENT

This study was supported by the Liaoning Provincial Science and Technology Plan Project, (2022JH1/10400017).

REFERENCES

[1] Bou Ali, G. (1993). *Straw bales and straw bale wall systems* (Master's thesis). Tucson, AZ, United States, The University of Arizona.

[2] Carrick, J., & Glassford, J. (1998). Vertical loading, creep, transverse loading, and racking loading on plastered straw-Bale walls, Sydney, Australia, *University of New South Wales*.

[3] Choi, Young, Lee, Chai-Sig, Lee, Jae-Sun. (2012). Comparison of Labor-Saving and Economical Efficiency on Mechanical Transplants of Ginseng Seeding. *The Journal of the Korean Society of International Agriculture*, Vol. 24, pp. 203–206, South Korea.

[4] Feng, T.X. et al. (2016) Optimization design and test research of plug seedings end-effector in greenhouse（温室末端执行器插拔播种的优化设计与试验研究）. *Beijing University of technology*, Beijing/China.

[5] Karayel, D., Canakci. M., Topakci. M., Aktas. A. (2023). Technical evaluation of transplanters' performance for potted seedlings. *Turkish Journal of Agriculture and Forestry*, Vol. 47, pp. 116–123, Turkey.
[6] King, B. (2003). Load-bearing straw bale construction. *Ecological Building Network*.
[7] Kornecki, TS., Kichler, C. (2022). Development of a No-Till Transplanter for Walk-Behind Tractors. *Applied Engineering in Agricultur*e. Vol. 38, pp. 865–872, United States of America.
[8] Luo, S. et al. (2018) Parameter calibration of discrete elemental method for vermicompost substrate based on JKR bonding model. (基于 JKR 粘结模型的蚯蚓粪基质离散元法参数标定). Journal of Agricultural Machinery.
[9] Liu, R. et al. (2022). Numerical Simulation of Seed-Movement Characteristics in New Maize Delivery Device. *Agriculture*, Vol.12, Issue 1944, Switzerland.
[10] Porteus, Sc., Parish, Rl., Wright, Me. (1988). A Mechanical Transplanter for Coastal Marsh Stabilization. *Louisiana Agriculture*, Vol. 31, pp. 12, United States of America.
[11] Rakowski, M. R. (2010). *Structural behaviour of plastered straw bale panels under non-uniform loading* (Doctoral thesis). Kingston.
[12] Walker, P., & Ay, B. (2004). Compression load testing straw bale walls. Bath, UK, *University of Bath*.
[13] Wang, Y. et al. (2022). Design of and Experiment on Reciprocating Inter-Row Weeding Machine for Strip-Seeded Rice. *Agriculture*, Vol.12, Issue 1956, Switzerland.
[14] Wen, Y.S. et al. (2020). Development of insertion and ejection type seedling taking device for vegetable plug seedlings（蔬菜穴盘苗插入顶出式取苗装置研制）. *Transactions of the Chinese Society of Agricultural Engineering*, Vol.36, Issue 22, pp. 96–104, Beijing/China.
[15] Yang, T, et al. (2017) Research on straw crushing technology and equipment（秸秆粉碎技术及设备的研究）. Sichuan Agriculture and Agricultural Machinery.
[16] Yan, D. et al. (2022). Soil Particle Modeling and Parameter Calibration Based on Discrete Element Method. *Agriculture*, Vol.12, Issue 1421, Switzerland.
[17] Yu, W.J. et al. (2020). Parameter Calibration of Pig Manure with Discrete Element Method Based on JKR Contact Model. *AgriEngineering*, Issue 2, pp. 367–377, Switzerland.
[18] Yu, X. et al. (2014) Current Situation and Prospect of Transplanter.（播秧机的未来与展望） *Transactions of the Chinese Society for Agricultural Machinery*, Issue 45, pp. 45–53, Beijing/China.
[19] Zhang, X., et al. (2022). The Design and Experiment of Vertical Variable Cavity Base Fertilizer Fertilizing Apparatus. *Agriculture*, Vol.12, Issue 1793, Switzerland.
[20] Zhou, L. et al. (2022). Analysis and Design of Operating Parameters of Floor-Standing Jujube Pickup Device Based on Discrete Element Method. *Agriculture*, Vol.12, Issue 1904, Switzerland.